

자기공명분석과 영상촬영을 위한 차폐된 고차경사자계코일의 설계

오창현^o, Sadek K. Hilal*, 이 윤, 김민기
고려대학교 자연과학대학 의용전자공학과

* Department of Radiology, Columbia University, New York, U.S.A.

Shielded High-Order Gradient Coil Design for Magnetic Resonance Spectroscopy and Imaging

Chang-Hyun Oh, Sadek K. Hilal*, Yun Yi, Min-Gi Kim
Department of Medical Electronics, Korea University, Korea

* Department of Radiology, Columbia University, New York, U.S.A.

ABSTRACT

High-order field gradients are useful for spatial localization of a volume of interest and dynamic range improvement of signal detection in NMR (Nuclear Magnetic Resonance) spectroscopy and imaging. This paper proposes a design method of shielded high-order gradient coils to reduce the effect of eddy current on the spectroscopy and imaging results. According to the experimental results, the shielded gradient coils produce less than 2 % eddy current compared to non-shielded coils. Two shielded z^2 gradient coils have been designed and constructed for 1.5 T whole-body and 3.0 T animal NMR imaging systems. Experimental results are in good agreement with the theoretically expected behavior and show the utility of the shielded high-order gradient coils.

INTRODUCTION

Recently, several useful techniques using pulsed high-order gradients have been proposed, i.e., dynamic range improvement methods by phase scrambling [1-3] and spatial localization methods using high-order gradients [4,5].

Since the magnetic field change due to the gradient pulsing may ruin the result of NMR spectroscopy or imaging by producing eddy current on the conductive part of the magnet, the active shielding for high-order gradient system will be very useful in using these techniques.

Although the basic principles of shielded gradient system for MRI is now well established [6-9] and can theoretically be used for any-order gradient coil systems, most of them have focused on

linear gradients. We have designed and implemented shielded " z^2 " (or " $z^2-(x^2+y^2)/2$ ") gradient coils and found that special consideration is needed for the design of high-order shielded gradient systems such as the suppression of both lower and higher order components than the necessary component while compensating for the effect of the shield. This is even more complex in the distributed-current system.

METHOD

The proposed design scheme uses a "component graph" for $[\partial^n B'_z(z)/\partial z^n]_{z=0}$ vs. z' , where z' is the position of the primary current loop and $B'_z(z)$ is the field from a single primary current loop and its corresponding shield.

The field intensity along the z-axis from one loop current can be expressed as

$$B_z(z, a, I, z') = \left(\frac{\mu_0 I}{2\pi} \right) \left[\frac{a^2}{\{a^2 + (z - z')^2\}^{\frac{3}{2}}} \right], \quad (1)$$

where μ_0 , I , a , z' , and z are the permeability of the free space, current, the radius and position of the loop current, and the field measurement position, respectively.

Equation (1) can be extended by including the continuous shield of one primary loop coil for a given shield radius, a' , as

$$B_z'(z, a, I, z') = B_z(z, a, I, z') + \int B_z(z, a', I'(z'' - z'), z'') dz'', \quad (2)$$

where $I(\cdot)$ is the shield current density as a function of the position relative to a single-loop primary current [6] and z'' is the shield current position. As an example, Fig. 1 shows B_z and B_z' as functions of the primary coil position (z') for $a=35$ cm and $a'=48$ cm. The graphs for B_z' (dotted line) show the shifted characteristics due to the addition of the shield compared to the graphs of B_z .

The z^n gradient coil design can be done by canceling out all the lower-order components and one higher-order component with the same symmetry.

Here it should be noted that the contribution of one loop coil to a specific component at $z=0$ can have different polarity depending on the coil position (z'). So, the polarity of coil position should be chosen carefully as a function of position when maximizing or canceling out a specific component. Gradient components for various orders are calculated from weighted integration under the graph depending on the current distribution of the primary coil.

RESULTS AND DISCUSSION

Figure 2 shows a design result of a shielded gradient system with distributed coil positions for a 1.5 Tesla whole-body clinical NMR imaging system. Here, the current distributions for the primary layer at the radius of 35 cm and the shield layer at the radius of 48 cm are optimized for the magnet inner conductive surface at the radius of 55 cm. From the continuous shield current distribution, discrete coil positions for a given current intensity are calculated. The current intensity through each wire is adjusted as a half of the primary current to make the distance between the adjacent shield current loops closer. The error caused by the truncation at each end and the approximation using discrete current loop element is minimized by iterative optimization of the coil positions. Although we have minimized the current intensity for a given gradient intensity (0.06 Gauss/cm²), other optimization methods such as minimization of the total power or inductance can also be adapted to this design method. The residual field intensity on the conductive magnet surface ($r=55$ cm) was less than 0.2 Gauss in this design for a primary loop current of 132 A.

Figure 3 shows another design results for a small-bore animal NMR imaging system. The primary current has two layers by winding a second layer on top of the first one. The wire current for the shield is the same as the primary in this case.

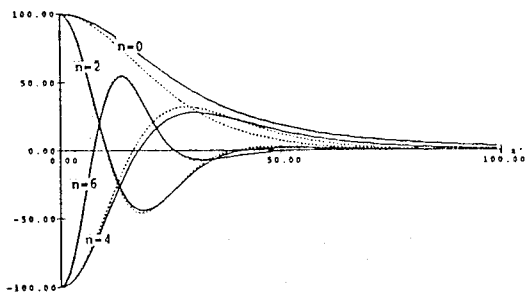


Fig. 1 Component graph : $[\partial^n B'_z(z)/\partial z^n]_{z=0}$ as a function of coil position z' for $n = 0, 2, 4,$ and 6 . (a) Solid lines : without shielding. (b) Dotted lines : with shielding.

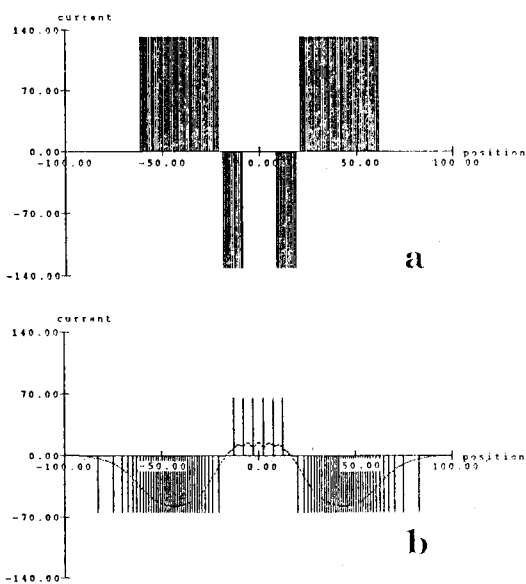


Fig. 2 Coil arrangement of a shielded z^2 gradient coil designed for a 1.5 Tesla whole-body NMR imaging system. z^0 and z^4 and all the odd components are canceled out. (a) Primary layer ($a=35$ cm). (b) Shield layer ($a'=48$ cm). The dotted line shows a continuous current distribution from which the discrete coil positions were derived.

The radii of the two primary layers and the shield layer are 5.134 cm, 5.295 cm, and 6.422 cm, respectively. For the wire diameter of 0.18 cm (minimum wire interval) and a given current intensity of 20 A, maximum of 3.0 Gauss/cm² of z^2 -gradient was obtained. The primary layers and shield layer have 144 (for two layers) and 72 windings, respectively. The conductive surface of the magnet was assumed to be at $r=11.5$ cm.

The above two coils have been constructed and tested experimentally. Two kinds of test results for the small-bore system are shown in this paper.

First we have tested the shielding effect by measuring the magnetic field. A sinusoidal waveform is applied to the coil and then B_z at $r=11.5$ cm was checked along the z -direction by measuring the induced voltage to a multi-layer solenoid (1 cm diameter and 1 cm length). The results are then calibrated to obtain B_z at $r=11.5$ cm from 10 A DC current. Three measurements were performed : (a) with only primary layer, (b) with both primary and shield layer, and (c) for the old unshielded z^2 gradient coil for reference (See Reference 4). The corresponding results are shown in Fig. 4(a), (b), and (c). By comparing (a) and (b), we can see the effectiveness of the active shielding. With the shield, B_z at $r=11.5$ cm was reduced to about 2% and this is close to the theoretical shielding effect obtained by simulation (1%). Figure 4(c), which is obtained by a non-shielded coil designed for only one primary layer, shows about half the B_z compared to (a). However, its maximum value was still more than 30 times bigger than the field in Fig. 4(b).

Another experiment was performed to see the effectiveness of active shielding by acquiring NMR signal from a 0.5 cc sample at the center of the magnet. A 5-msec-long 13-Ampere-high pulse was applied (with 200 μ s rise and fall times) right before a 90° RF excitation pulse. The FID (Free Induction Decay) signal was measured without, (b), and with, (c), the shield and compared with the FID obtained without gradient pulsing, (a). As expected, a large amount of eddy current produced by gradient pulsing affected the field at the center when the shield is not used. The acquired FID shows frequency modulation due to the temporary magnetic field change, specially near $t=0$ msec. However, when the shield is connected, there is almost no change in FID shape compared to Fig. 5(a) showing the effectiveness of active shielding.

CONCLUSION

According to the simulation and the experimental test results, the shielded high-order gradient coil seems to be very useful for NMR spectroscopy or imaging, specially for the applications where the results are sensitive to the eddy current from gradient pulsing, such as spatial volume selection for localized NMR spectroscopy.

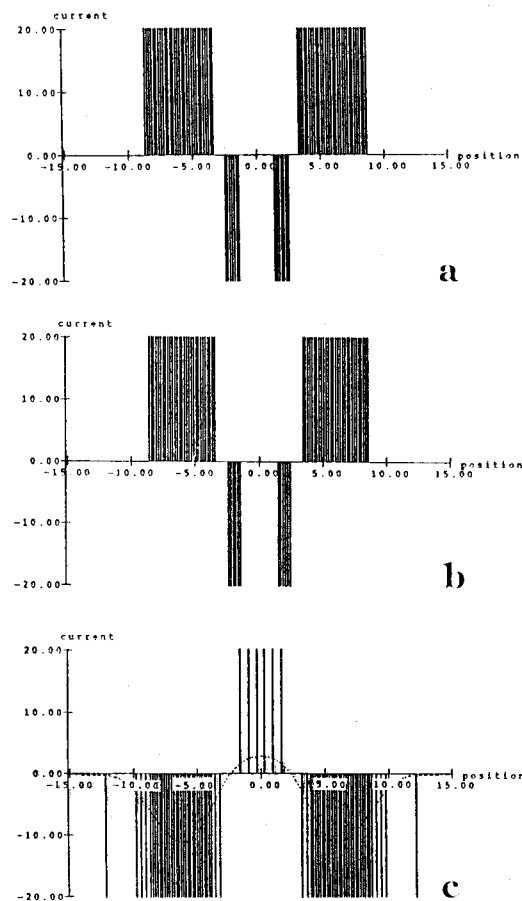


Fig. 3 Design results for a 3.0 Tesla small-bore system with two primary layers and one shield layer. (a) Primary layer I ($r=5.134$ cm). (b) Primary layer II ($r=5.259$ cm). (c) Shield layer ($r=6.422$ cm).

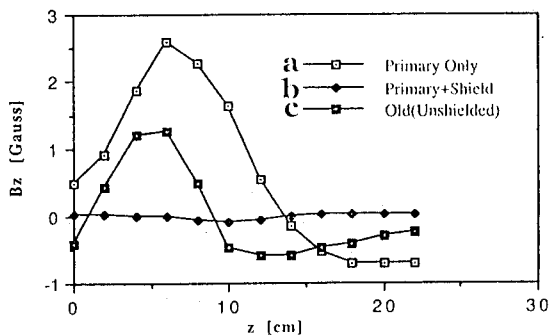


Fig. 4. Experimentally measured B_z at $r=11.5$ cm for the coil current of 10 A. (a) With only primary layer. (b) With both primary and shield layers. (c) For a non-shielded z^2 gradient coil.

REFERENCES

1. A.A. Maudsley, "Dynamic range improvement in NMR imaging using phase scrambling," *J. Magn. Reson.*, vol. 76, p. 287, 1988.
2. C.H. Oh, S.K. Hilal, G. Johnson, I.K. Mun, Z.H. Cho, "Spectral resolution enhancement in NMR by phase scrambling," *Proc. SMRM VIII*, p. 925, 1989.
3. C.H. Oh, S.K. Hilal, E.X. Wu, Z.H. Cho, "Phase-scrambled RF excitation for 3D volume-selective multislice NMR imaging," *Magn. Reson. Med.*, vol. 28, p. 290, 1992.
4. C.H. Oh, S.K. Hilal, Z.H. Cho, I.K. Mun, "New spatial localization method using pulsed high-order field gradients (SHOT: Selection with High-Order gradient)," *Magn. Reson. Med.*, vol. 18, p. 63, 1991.
5. C.H. Oh, S.K. Hilal, I.K. Mun, Z.H. Cho, "Radial encoding by using high-order gradients," *Proc. SMRM IX*, p. 1079, 1990.
6. P. Mansfield, B. Chapman, "Active magnetic screening of gradient coils in NMR imaging," *J. Magn. Reson.*, vol. 36, p. 573, 1986.
7. R. Turner, R. M. Bowley, "Passive screening of switched magnetic field gradients," *J. Phys. E: Sci. Instru.*, vol. 19, p. 876, 1986.
8. P. Mansfield, B. Chapman, "Multishield active screening of coil structures in NMR," *J. Magn. Reson.*, vol. 72, p. 211, 1987.
9. J.W. Carlson, "An optimized, highly homogeneous shielded gradient coil design," *Proc. SMRM VII.*, p. 28, 1988.

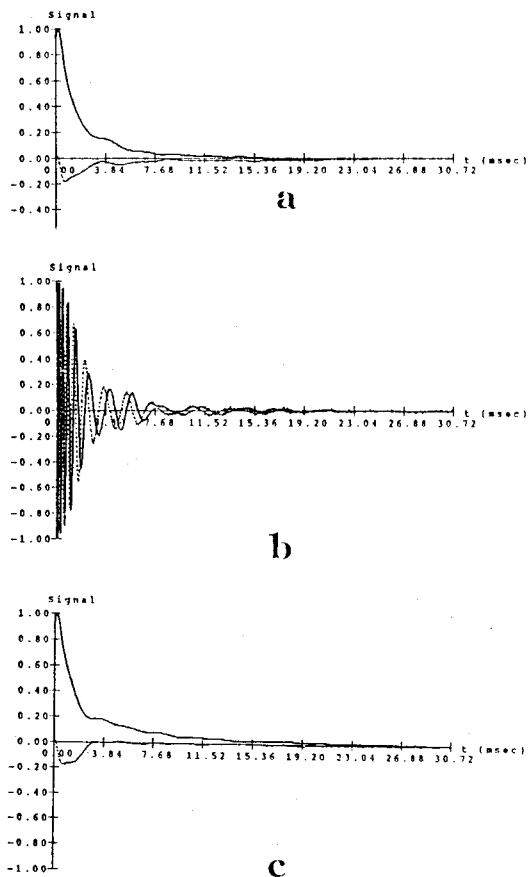


Fig. 5 FID signal from a small sample at the magnet center. (a) Without gradient pulsing. (b) With gradient pulsing (without the shield layer). (c) With gradient pulsing (with the shield layer).